Phytochemistry 148 (2018) 1–10

Contents lists available at ScienceDirect

Phytochemistry

journal homepage: www.elsevier.com/locate/phytochem

Cadopherone and colomitide polyketides from *Cadophora* wood-rot fungi associated with historic expedition huts in Antarctica

Yudi Rusman [a], Benjamin W. Held [b], Robert A. Blanchette [b], Yanan He [c], Christine E. Salomon [a, *]

[a] Center for Drug Design, University of Minnesota, Minneapolis, MN, United States
[b] Department of Plant Pathology, University of Minnesota, Saint Paul, MN, United States
[c] BioTools, Jupiter, FL, United States

ARTICLE INFO

Article history:
Received 16 May 2017
Received in revised form
25 December 2017
Accepted 29 December 2017

Keywords:
Polyketide
PKS
Colomitide
Spiciferone
Cadopherone
Similin
Fungus
Cadophora

ABSTRACT

Recent investigations of filamentous fungi isolated from coastal areas and historic wooden structures in the Ross Sea and Peninsula regions of Antarctica have identified the genus *Cadophora* as one of the most abundant fungal groups, comprising more than 30% of culturable fungi at some locations. A methanol extract of *Cadophora luteo-olivacea* grown on rice media yielded the known polyketides spiciferone A, spiciferol A, dihydrospiciferone A and dihydrospiciferol A. Additionally, nine related hexaketides were identified, including spiciferone F, two isomers of the known fungal bicyclic ketal colomitide B, cadopherones A-D, similin C, and spicifernin B. HPLC and NMR analysis of extracts from other isolates collected in Antarctica suggests that the spiciferones and colomitides are produced by at least two different *Cadophora* species. Preliminary precursor feeding experiments provided evidence for the biosynthesis of the colomitides from the same polyketide pathway as the spiciferone phytotoxins, possibly via a type III polyketide synthase (PKS). None of the compounds were active in a panel of anti-bacterial, anti-fungal, and mammalian cytotoxicity assays.

1. Introduction

Members of the *Cadophora* genus of fungi are found throughout the world and are responsible for a small number of agricultural diseases such as lesions on grapevines, pear rot, and necrosis of kiwifruit (Spadaro et al., 2010; Sugar and Spotts, 1992; Travadon et al., 2015). Recent studies of filamentous fungi isolated from coastal areas and historic wooden structures in the Ross Sea and Peninsula region of Antarctica as well as historic structures at Deception Island have identified this genus as one of the most abundant groups, comprising more than 30% of culturable fungi at some locations (Arenz and Blanchette, 2009; Blanchette et al., 2010). Several *Cadophora* species, including *C. luteo-olivacea* were found to cause a soft rot form of wood decay in the Ross Sea historic expedition huts, in wood from historic structures at Deception Island, and on the Peninsula of Antarctica (Arenz and Blanchette, 2009; Blanchette et al., 2004; Held et al., 2011). *Cadophora* has also been found associated with decaying wood in the Arctic (Blanchette et al., 2008; Jurgens et al., 2009). Despite the global distribution of the genus, *Cadophora* species have been rarely studied for the production of novel secondary metabolites (Almeida et al., 2010; Rusman et al., 2015). Due to the unusual abundance of these species in polar areas and their significant role in wood decay in extreme environments, this study was undertaken to explore the structural diversity and biological activities of compounds from *Cadophora* isolates collected from several historic structures from different regions of Antarctica.

Fractionation of the methanol extract of *Cadophora luteo-olivacea* (UMN PL12-3) collected from Port Lockroy on the Antarctic peninsula led to the identification of the known polyketides spiciferone A (**1**) (Nakajima et al., 1989), spiciferol A (**2**) (Edrada et al., 2000), the first isolation of dihydrospiciferone A (**3**) from nature, dihydrospiciferol A (**4**) and new congeners spiciferone F (**5**), colomitides C (**6**) and D (**7**), cadopherones A-D (**8**–**11**), similin C (**12**) and spicifernin B (**13**) (Fig. 1). HPLC analysis of extracts from other species of *Cadophora* collected in Antarctica demonstrated that the

* Corresponding author. Center for Drug Design, University of Minnesota, 312 Church St. SE, Minneapolis, MN, 55455, United States.
E-mail addresses: rusma002@umn.edu (Y. Rusman), bheld@umn.edu (B.W. Held), robertb@umn.edu (R.A. Blanchette), yanan.biotools@gmail.com (Y. He), csalomon@umn.edu (C.E. Salomon).

https://doi.org/10.1016/j.phytochem.2017.12.019
0031-9422/

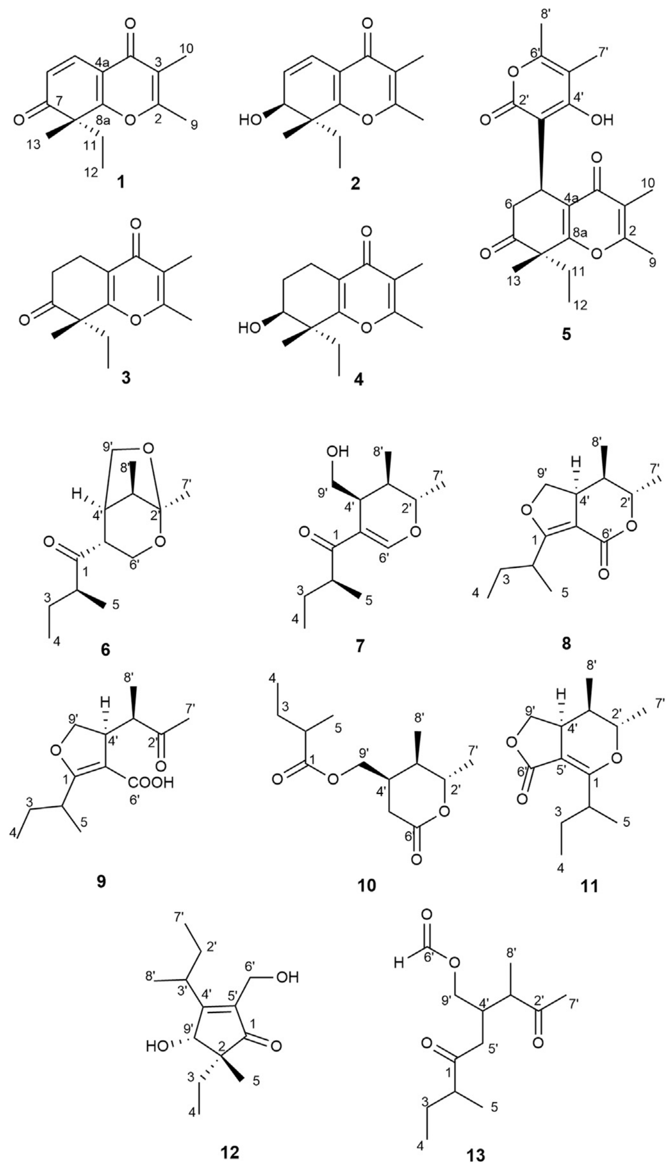

Fig. 1. Structures of compounds **1**–**13**.

spiciferones and colomitides are produced by members of at least two distinct species collected from geographically distant locations. These results in combination with previous reports of colomitide derivatives from other fungal genera collected from diverse locations including freshwater and marine species suggest that the same polyketide pathway may be widespread among many fungal groups globally.

The similar structural features between the spiciferones and colomitide compounds also led to consideration of their biosynthetic relationships. Preliminary labeled precursor feeding experiments together with previously reported biosynthetic studies provided evidence for a core polyketide chain assembly and aromatic intermediates to construct a diverse suite of related compounds. None of the new compounds were active in a panel of antibacterial, anti-fungal and mammalian cell cytotoxicity assays.

2. Results and discussion

2.1. Isolation and structure elucidation

Compound **3** was isolated as a white solid with a molecular formula of $C_{14}H_{18}O_3$ deduced from the HRAPCI-MS peak at *m/z* 235.1347 ($[M+H]^+$). Analysis of the 1-D and 2-D NMR data suggested that the structure was similar to the phytotoxic γ-pyrone spiciferone A (**1**), first isolated from the wheat leaf spot fungal pathogen *Cochliobolus spicifer* (Nakajima et al., 1989). The absence of the C-5/C-6 alkene signals in the ^1H NMR spectrum and the additional two protons in the molecular formula provided support for the identification of compound **3** as dihydrospiciferone A, and all of the spectroscopic data matched published values. Dihydrospiciferone A was previously reported as a semi-synthetic derivative produced by hydrogenation of spiciferone A (**1**) for structure/activity studies (Nakajima et al., 1993a). A closely related analog (**4**) was also isolated and found to have a molecular formula of $C_{14}H_{20}O_3$. Comparison of the spectroscopic data of **4** to literature values confirmed the structure as dihydrospiciferol A, previously isolated from the fungus *Pestalotiopsis disseminata* (Hwang et al., 2016) and also reported as a derivative produced by chemical reduction of dihydrospiciferone A (Hwang et al., 2016; Nakajima et al., 1993a).

Compound **5** was obtained as a white solid with a formula of $C_{21}H_{24}O_6$ (ten degrees of unsaturation) determined by HRAPCI-MS. The ^1H NMR spectrum included signals for two pairs of methylenes, one methine, five singlet methyls, and one triplet methyl group (Table 1). Analysis of the 2D NMR data suggested the presence of a substituted dihydrospiciferone A (**3**) unit with a sidechain 4-pyranone moiety in the molecule as described below. The HMBC correlations of two vicinal methyls (CH_3-8′ and CH_3-7′) to non-protonated sp^2 carbons at δ_C 157.7 (C-6′) and δ_C 109.4 (C-5′), as well as correlations of a hydroxyl group (δ_H 12.35) to carbons at δ_C 168.1 (C-4′) and δ_C 103.8 (C-3′) indicated the position of two double bonds in the pyranone ring. The linkage of the pyranone subunit to the main dihydrospiciferone core at C-5 was established by HMBC correlations of H-5, H-6a, and H-6b to C-3′, and of H-5 to C-2′ and C-4′. The relative configuration was determined by observation of NOE correlations of CH_3-12 to H-6b (pseudoaxial), the $J = 7.5$ Hz between H-5 and H-6b and lack of *J*-coupling between H-5 and H-6a suggesting a dihedral angle close to 90° (Fig. 2). Compound **5** is a new member of the spiciferone family of compounds and was given

Table 1
^1H and ^{13}C data for **5** ($CDCl_3$, δ in ppm and *J* in Hz).

Position	**5**	
	δ_H	δ_C
1		
2		164.1
3		118.2
4		180.0
4a		119.6
5	4.40 d (7.5)	26.8
6	a 2.79 d (15.0) b 2.61 dd (15.0, 7.5)	43.2
7		207.5
8		51.0
8a		167.0
9	2.37 s	18.1
10	1.99 s	9.8
11	a 1.92 m b 1.90 m	34.4
12	0.71 t (7.7)	9.9
13	1.70 s	23.0
2′		165.2
3′		103.8
4′		168.1
5′		109.4
6′		157.7
7′	1.94 s	10.0
8′	2.13 s	17.1
4′ OH	12.35 s	

the trivial name spiciferone F.

Compound **6** was obtained in high yields (>1 g/kg rice medium) as a volatile, colorless oil with a molecular formula of $C_{13}H_{22}O_3$ based on analysis of the HRAPCI-MS pseudomolecular ion peak at *m/z* 227.1653. The ^{1}H and HMQC spectra indicated the presence of four methyls, three methylenes and four methine groups. An acetal unit in the molecule was identified by the HMBC correlations of H_2-6′, H_2-9′, H-3′, H-4′, CH_3-7′ and CH_3-8′ to a doubly oxygenated sp^3 carbon at δ 110.1 (C-2′). HMBC correlations of CH_3-5, H-2, H_2-3, and H_2-6′ to a ketone carbonyl at δ 216.3 (C-1), as well as correlations of H-2 to C-5′ (δ 54.0) indicated the presence of a 2-methylbutanone side chain and its link to C-5′ in the ring system. Comparison of the structural data to literature values revealed that the 2-dimensional structure of **6** was the same as colomitides A and B (Fig. 3), diastereoisomeric bicyclic ketals isolated from an unidentified fungus (Dong et al., 2009). The gross structure of compound **6** is also similar to disseminin B, an analog isolated from *Pestalotiopsis disseminata* with an additional hydroxyl group at C-3. Careful analysis of the NOE data and *J*-values for **6** established the same relative configuration of the five stereocenters as for colomitide B (Fig. 3), but the specific rotation was a positive value (**6** $[\alpha]_D^{25} = +26$, colomitide B $[\alpha]_D^{20.9} = -23$) suggesting the opposite absolute stereochemistry. To determine the absolute configuration, **6** was analyzed by Vibrational Circular Dichroism (VCD) spectroscopy. Due to the requirement that the chiral centers at C-2′ and C-4′ must be set by the bridged system, there are 16 possible configurations. Since half of these structures are enantiomers of each other, the theoretical spectra for eight of the possible diastereomers were calculated by Compute VOA (Fig. S14). For each of the calculated configurations, conformers resulting from Gaussian calculations with energies within 1.5 kcal/mol from the lowest-energy conformers were selected to generate the Boltzman-averaged IR and VCD spectra. Comparison of the observed spectra to those of the calculated configurations (Fig. 4 and Fig. S14) established the absolute configuration of **6** as *2S2′S3′R4′S5′R* and the proposed trivial name is colomitide C. Recently, the synthesis of colomitides A-C was reported (Yang et al., 2017), and the specific rotation, proton and carbon NMR data for natural colomitide C compared to the synthetic version are nearly identical (Table S1), further supporting the configuration assignments. Notably, the C-2 epimer of colomitide C was also synthesized, and its specific rotation was reported as $[\alpha]_D^{21.3} = -6.2$ (*c* 0.45, acetone) vs. synthetic colomitide C $[\alpha]_D^{18} = +22.5$ (*c* 0.39, acetone).

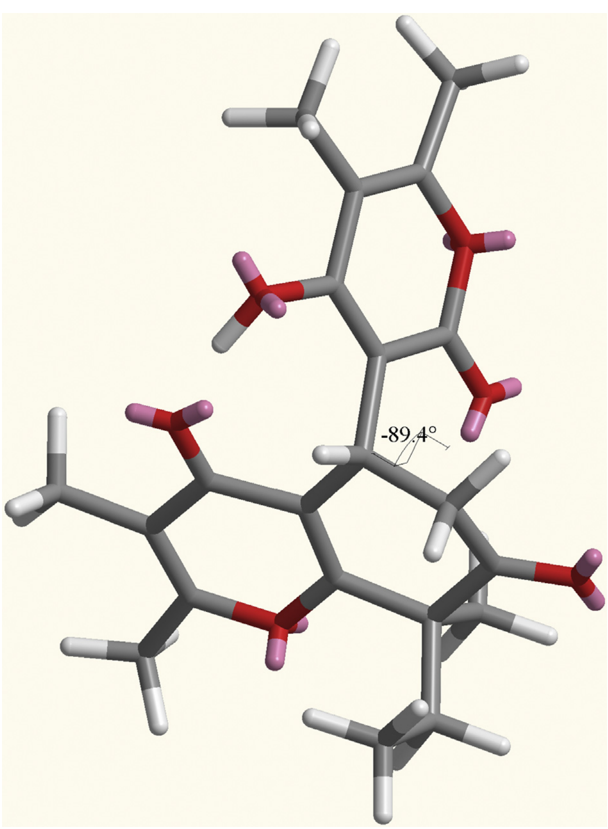

Fig. 2. Energy minimized drawing of **5**.

Compound **7** was isolated as an isomer of **6** with a molecular formula of $C_{13}H_{22}O_3$. Comparison of the ^{1}H NMR spectra showed that they are structurally related, but the spectrum for **7** included a downfield doublet at δ_H 7.90 suggestive of an oxygenated olefin unit. The position of the double bond and the dihydro-*2H*-pyran ring was confirmed by HMBC correlations of H-6′ to C-1, C-2′, C-4′ and C-5′, as well as correlations of H-3′, H_2-9′, and H-2 to C-5′. The 2-methyl butanone side chain attached to C-5′ was established by HMBC correlations from H-2, CH_3-5, H_2-3, and H-6′ to the ketone carbon C-1. Since all three double bond equivalents were accounted for (ketone, dihydropyran and olefin), the structure of **7** was recognized as a monocyclic analog of **6**. This observation was supported by a hydroxymethyl group at C-4′ (H_2-9′, δ_H 3.61) and new methine proton signal at C-2′ (δ_H 4.26). The relative configurations of C-2′, C-3′ and C-4′ were determined by NOE correlations of H-2′ to H_2-9′ and CH_3-8′ and are consistent with the configurations assigned for colomitide C. The configuration of C-2 was not determined, but assumed to be the same as for **6**. Compound **7** is similar to the 2-dimensional structures of the previously reported disseminins C-E from the fungus *P. disseminata*, but differs in the configurations at C-3′ and C-4′ (Hwang et al., 2016). Given the likely biosynthetic relationship to colomitide C, **7** was given the trivial name colomitide D.

Analysis of the HRAPCI-MS data for **8** revealed a pseudomolecular ion peak at *m/z* 225.1484 $[M+H]^+$, consistent with a molecular formula of $C_{13}H_{20}O_3$ (four degrees of unsaturation). The proton NMR spectrum indicated three doublet methyls, one triplet methyl, and three protons attached to oxygenated carbons suggesting a structural similarity to **6** and **7**. In the HMBC spectrum, the loss of the ketone signal (C-1, as in **6** and **7**) and replacement by a non-protonated sp_2 carbon at δ_C 179.6 with a correlation to H_2-9′ suggested the presence of a dihydrofuran ring system in the molecule. The position of a *sec*-butyl side chain was determined by HMBC correlations of H-2, H_2-3 and CH_3-5 to C-1 (δ_C 179.6) and H-2 to C-5′ (δ_C 97.3). In addition, the HMBC correlations of H-2′ and H-4′ to an additional ester carbonyl at δ_C 166.2 (C-6′) corroborated the presence of an adjacent δ-lactone ring incorporating C-2′ and C-6′. The relative configurations of C-2′, C-3′, and C-4′ were determined by observations of NOE correlations of H-9′b to CH_3-8′ and H-4′ to CH_3-7′. The configuration of C-2 was not determined, but is predicted to be *S* based on the shared biosynthetic relationship between **8** and related compounds such as **6**. The proposed trivial name for bicyclic lactone **8** is cadopherone A.

Compound **9** was isolated as a colorless oil with a molecular formula of $C_{13}H_{20}O_4$ deduced from the HRESI-MS data showing a peak at 239.1274 [M-H]- (four degrees of unsaturation). Analysis of the 1D and 2D NMR data indicated a similar substituted dihydrofuran ring system as in **8**. A butan-2-one side chain at C-4′ was identified by the presence of a downfield ketone signal at δ_C 211.5 (C-2′) with HMBC correlations to CH_3-7′, CH_3-8′, and H-4′. The presence of an additional carbonyl signal (C-6′, δ_C 171.3) which only correlates to H-4′ in the HMBC spectrum suggested the presence of a free carboxylic acid at position C-5′. The monocyclic structure of **9** was therefore identified as a ring-opened monocyclic analog of **8**,

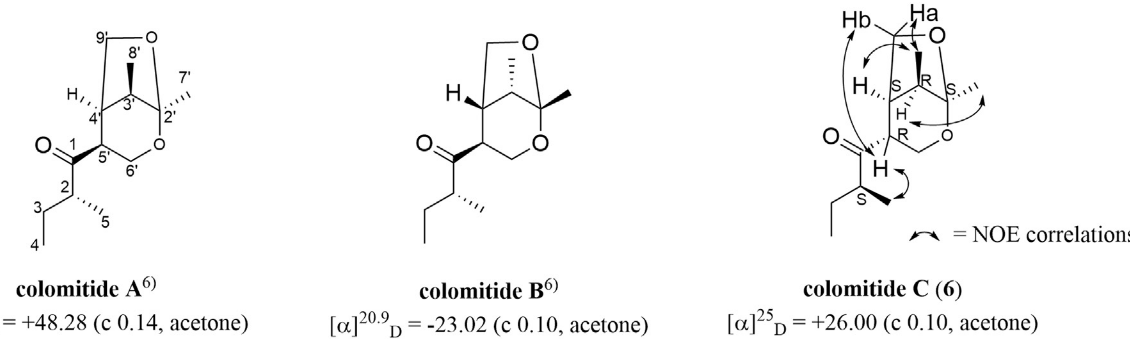

Fig. 3. Comparison of stereochemical configurations of colomitides A-C and NOE correlations observed for colomitide C (**6**).

and given the name cadopherone B. The relative configuration of C-4′ is consistent with the assignment identified for compound **8** based on analysis of the J coupling and NOE correlation data. The configuration of C-3′ could not be determined by NMR analysis but is assumed to be the same as for compound **8**. The configuration of C-2 was not determined.

Compound **10** was afforded as a white solid with a molecular formula of $C_{13}H_{22}O_4$ (3 degrees of unsaturation) deduced from the HRAPCI-MS pseudomolecular ion peak at *m/z* 243.1585 $[M+H]^+$. The NMR spectra were similar to those for **8** and **9**, but differed in the absence of the C-5′/C-1 double bond signals and addition of new methylene signals for H_2-5′. HMBC correlations of H-9′a, H-2, H-3a and CH_3-5 to a carbonyl at δ_C 178.2 (C-1) revealed the ester linkage of a 2-methyl butanoate side chain at C-4′. HMBC correlations of the methylene protons at C-5′ (δ_H 2.65 and δ_H 2.49) to a second ester carbonyl at δ_C 174.4 (C-6′) provided additional evidence for monocyclic lactone **10**. The relative configurations of C-2′, C-3′ and C-4′ were determined by analysis of NOE correlations of CH_3-8′ to H-2′ and H-9′a/9′b and between CH_3-7′ and H-2′. The proposed trivial name for **10** is cadopherone C.

Compound **11** was isolated as an isomer of **8** with the same molecular formula. The NMR data were similar and indicated the same spin system between C-2′ and C-9′. However, some notable differences included an upfield shift for the ester carbonyl (C-6′,δ_C 172.4) which displayed HMBC correlations to H-4′ and H_2-9′ methylene protons indicating a γ-lactone ring. Evidence for a fused dihydropyran ring was provided by an HMBC correlation of H-2′ to oxygenated olefin carbon C-1 (δ_C 168.2). A *sec*-butyl side chain was indicated by HMBC correlations of H-2, H_2-3, CH_3-5, H-2′ and H-4′ to C-1 and also confirmed its attachment at C-1. An NOE correlation between H-4′ and CH_3-7′ indicated their positions on the same face of the dihydropyran ring, and the correlation between CH_3-8′ and H-9′b indicated their position on the opposite face of the ring system. The configuration of C-2 was not determined. Compound **11** was given the name cadopherone D.

Analysis of the HRAPCI-MS data for **12** revealed a pseudomolecular ion peak at *m/z* 227.1647 $[M+H]^+$ consistent with a molecular formula of $C_{13}H_{22}O_3$ (three degrees unsaturation). HMBC correlations of H_2-6′ and CH_3-5 to a carbonyl signal at δ_C 209.7 established the ketone at C-1. The presence of geminal ethyl and methyl groups at C-2 was indicated by HMBC correlations of their protons to C-2 and correlations of H_2-3 and CH_3-5 to the C-1 ketone and oxygen-bearing carbon at C-9′. HMBC correlations of H-3′, H_2-2′, and CH_3-8′ to the downfield shifted olefin carbon at C-4′ established a *sec*-butyl side chain at C-4′. The double bond position at C-4′/C-5′ was supported by HMBC correlations of H_2-6′ and H-3′ to C-5′ and C-4′. The relative configuration of C-9′ was determined by the NOE correlation of H-9′ to CH_3-5. The relative configuration of C-3′ could not be determined. Compound **12** is the C-9′ alcohol derivative of the known antifungal polyketide similin A isolated from the coprophilous fungus *Sporomiella similis* and was given the trivial name similin C (Weber et al., 1992).

The molecular formula $C_{13}H_{22}O_4$ (three degrees of unsaturation) of **13** was determined by analysis of the HRESI-MS pseudomolecular ion peak at *m/z* 243.1608. HMBC correlations of CH_3-7′, CH_3-8′ and H-4′ to a carbonyl at δ_C 214.2 (C-2′) confirmed the presence of a 3-substituted-2-butanone unit as in compound **9**. Analysis of the COSY spectrum revealed the presence of one spin system consisting of H-3′ through H-5′, CH_3-8′ and H_2-9′ and an additional

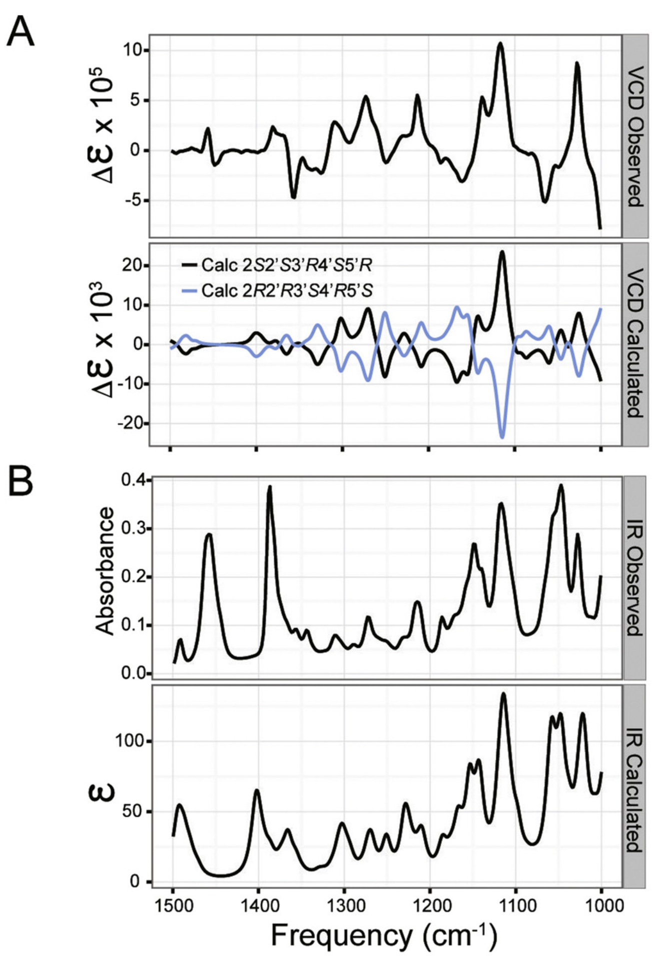

Fig. 4. VCD (upper frame) and IR (lower frame) spectra observed for colomitide C (**6**), (right axes) compared with the calculated Boltzmann-averaged spectra for the *2S2′S3′R4′S5′R* and 2R2′R3′*S4′R5′S* configurations.

isolated spin system consisting of CH_3-4, H_2-3, H-2, and CH_3-5. These two spin systems were linked to each other via a ketone carbon at δ_C 215.5 (C-1) as shown by HMBC correlations to H-4′, CH_3-5 and H_2-3. A formate moiety at C-9′ was identified by HMBC correlations of H_2-9′ and formyl group proton (H-6′, δ_H 8.06) to an upfield carbonyl at δ_C 163.1. Compound **13** is the only new acyclic compound isolated during this study and differs from the previously reported plant growth regulator spicifernin by the presence of a methyl formate group instead of a carboxylic acid at C-4′ and the lack of an acetate moiety at C-2 (Nakajima et al., 1990). The configurations of the three stereocenters could not be determined by standard NMR techniques. The proposed trivial name for compound **13** is spicifernin B.

2.2. Biological activity

Compounds **1**, **2**, **3**–**11** and **13** were tested for antimicrobial activities using a broth dilution assay against methicillin-resistant *Staphylococcus aureus* (MRSA), vancomycin-resistant *Enterococcus faecalis* (VRE), *Bacillus subtilis*, *Escherichia coli*, *Acinetobacter baumannii*, *Pseudomonas aeruginosa*, *Klebsiella pneumoniae*, *Cryptococcus neoformans* and *Candida albicans*. These compounds were also tested for cytotoxicity against LOX IMVI (melanoma) and SF-295 (glioblastoma) human cancer cell lines using an MTT viability assay. None of the compounds were inhibitory towards any of the tested bacterial or fungal pathogens (MIC > 50 μg/mL) or cancer cells (IC_{50} > 50 μM).

2.3. Biosynthetic studies

The compounds isolated during this study are structurally related to several groups of metabolites previously identified from different fungal genera. The spiciferones and spicifernin were first reported from *Cochliobolus spicifer* and found to have phytotoxicity and plant growth promotion activity, respectively (Nakajima et al., 1989, 1990). Spiciferones and related derivatives were also identified from the fungus *Drechslera hawaiiensis* isolated from a marine sponge (Edrada et al., 2000). The bridged colomitide polyketides were first isolated from an unidentified fungus cultivated from wood collected from a freshwater mangrove and exhibited moderate anti-bacterial activities (Dong et al., 2009). Several spiciferone and colomitide analogs (disseminins) were recently isolated from *Pestalotiopsis disseminata* (Hwang et al., 2016) and are postulated to arise from the same polyketide precursor. The isolation of both spiciferones and colomitides from *C. luteo-olivacea* in this study and common structural features further support a possible common biosynthetic pathway. A preliminary feeding study was conducted using 1–^{13}C and 2–^{13}C labeled acetate to explore the biogenic relationship between the colomitides and spiciferones. Similar studies were previously used to propose biosynthetic pathways for spiciferone A, spiciferinone, and spicifernin involving a linear hexaketide and multiple cyclization, cleavage and tailoring steps (Nakajima et al., 1992, 1993b, 1994). However, in contrast to the pathway proposed by Nakajima et al., (1993b), an alternative hypothesis is that the spiciferones, spiciferinone, spicifernin, colomitide (**6**) and its monocyclic derivative **7** are produced via a type III PKS pathway. A branched polyketide chain formed from incorporation of malonate and ethylmalonate is cyclized into one of two possible aromatic intermediates (Fig. 5). Although butyryl moieties are known to be incorporated into a number of polyketides synthesized by type I PKSs, ethylmalonyl-CoA is a rare extender unit in type III PKS pathways (Chan et al., 2009; Song et al., 2006). Feeding of ^{13}C-2 labeled sodium acetate to a culture of *C. luteo-olivacea* resulted in a relative enrichment of the carbon signals at C-2, C-4, C-3′, C-5′, C-7′, and C-9′, and additions with ^{13}C-1 acetate resulted in enrichments at positions C-1, C-3, C-2′, C-4′, and C-6′, consistent with the proposed biosynthetic route (Figs. 5 and 6, Table 5). Carbons at C-5 and C-8′ were not labeled under either condition, and are presumed to originate from S-adenosyl methionine (SAM) as previously demonstrated for the analogous positions in spiciferone A and spicifernin (Nakajima et al., 1993b). Additional feeding studies and whole genome sequence analysis are in progress to further elucidate the biosynthetic pathways for all of the related polyketides produced by *C. luteo-olivacea.*

Since different species of the genus *Cadophora* are abundant throughout polar regions, other isolates collected from different geographic locations in Antarctica were analyzed for the production of spiciferones and colomitides. Isolates of *C. malorum* (UMN Di3-4) and *C. fastigiata* (UMN Di76-3) isolated from Deception Island were cultured and extracted using identical conditions as for *C. luteo-olivacea*. An additional isolate of *C. luteo-olivacea* (UMN 3E41-2) collected from a geographically distant location (Ross Island) was also extracted. The extracts were subjected to liquid/liquid partitioning and the EtOAc fractions were analyzed by HPLC and ^{1}H NMR. Comparison of the extract fractions with the original *C. luteo-olivacea* producer and pure samples of colomitide C and spiciferone A demonstrated that both compounds were also produced by the second *C. luteo-olivacea* and *C. malorum*, but not *C. fastigiata* (Figs. S66–S67). These results together with previous reports of spiciferones and colomitides from diverse fungal genera suggest that this polyketide biosynthetic pathway may be distributed among multiple fungal groups globally.

Although previous research has demonstrated the likely role of spiciferones and spicifernin in mediating phytotoxicity and plant growth promotion, respectively, the ecological role of the most abundant *C. luteo-olivacea* compound colomitide C (**6**) remains unknown. The lack of any significant anti-microbial or cytotoxic activities suggests that it is probably not involved in antagonism or defense, although it is important to note that assays were done with standard human pathogens and not ecologically relevant species. The volatile nature of colomitide C may aid in dispersal and provide a means for functioning as a chemical signal in terrestrial environments. Similar volatile heterobicyclic compounds such as frontalin and brevicomin are produced by pine beetles as signaling pheromones (Kinzer and Fentiman, 1969; Silverstein et al., 1968), but is it not yet known if the colomitides play a role in mediating any species interactions in microbial communities or in association with plants. The production of phytotoxic spiciferone compounds among multiple species of *Cadophora* collected from different geographic areas of Antarctica is also interesting given the absence of vascular plants on the continent. Further research will be needed to determine their ecological targets as well as the levels of production under natural conditions *in situ*.

3. Conclusions

Nine new hexaketides including spiciferone F, colomitides C and D, cadopherones A-D, similin C, and spicifernin B together with four previously identified spiciferone analogs were identified from a rice culture of an Antarctic isolate of the fungus *Cadophora luteo-olivacea*. A stable isotope feeding study with ^{13}C labeled acetate provided data that support the biosynthesis of both colomitides and spiciferone metabolites from the same core type III polyketide synthase (PKS) pathway. None of the compounds were inhibitory against a panel of cancer cell lines or microbial pathogens. More research is needed to determine if the production of the isolated compounds play any roles in the growth or competitiveness of *Cadophora* spp. fungi in polar environments.

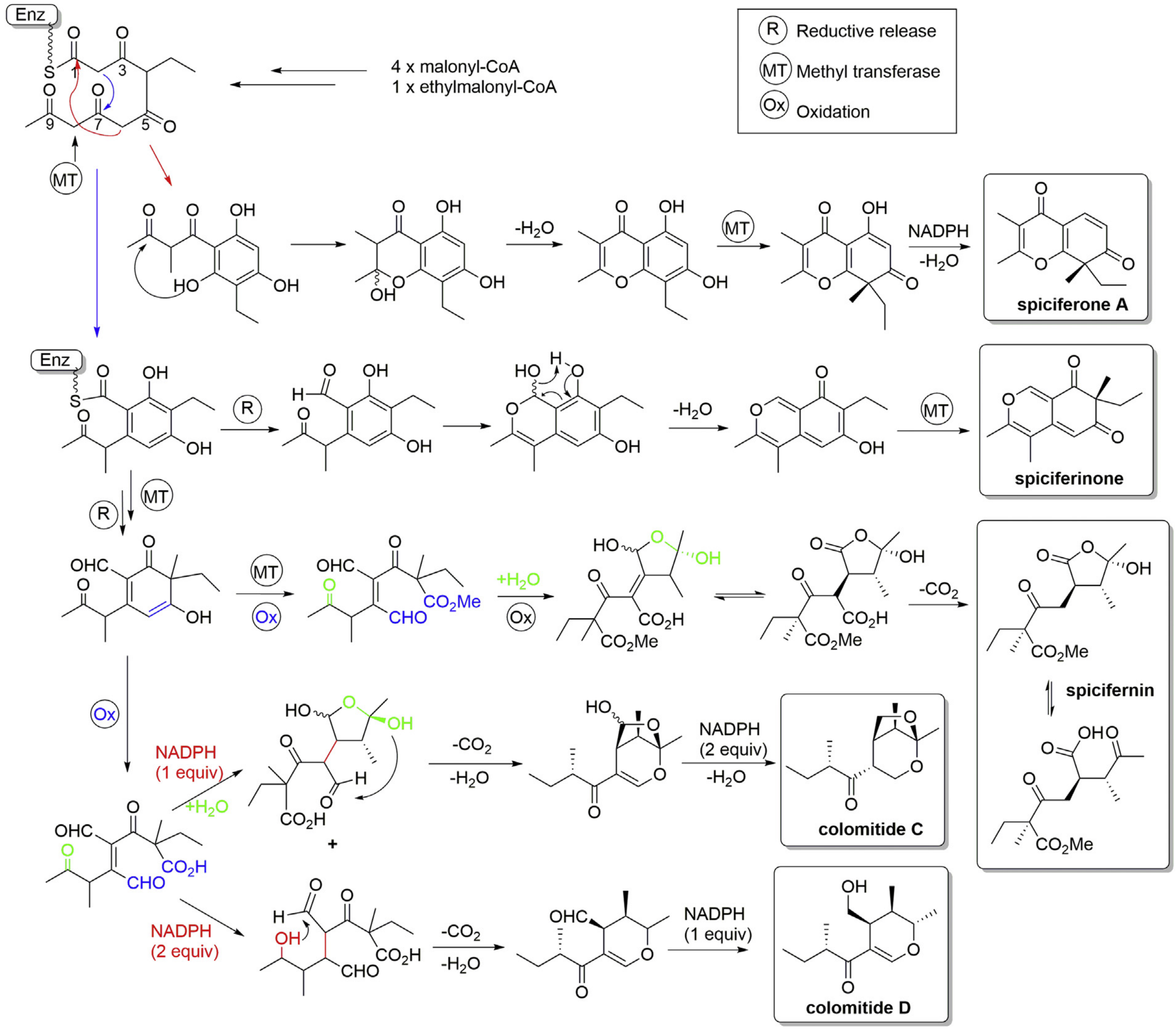

Fig. 5. Proposed biosynthesis of colomitides and biogenic relationship to spiciferone A, spiciferinone and spicifernin polyketides.

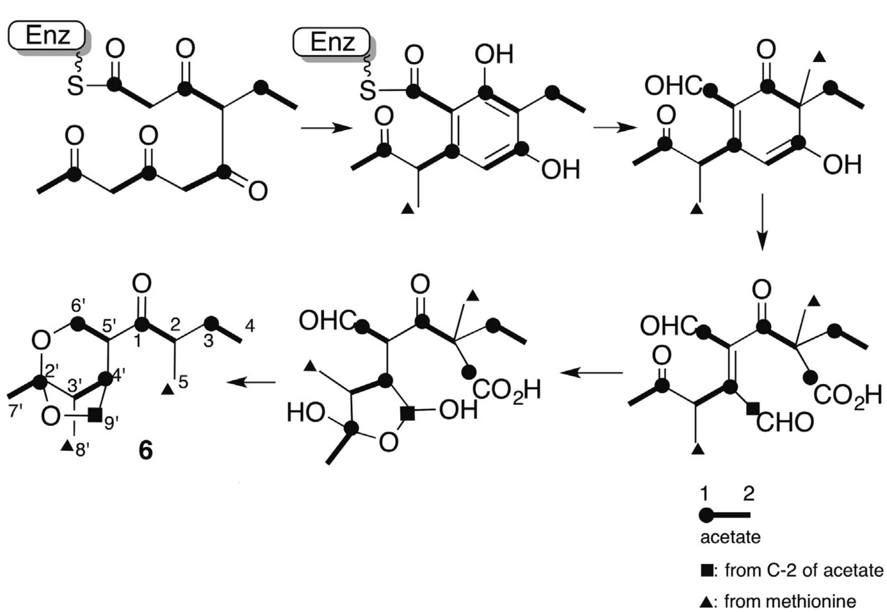

Fig. 6. Predicted incorporation of ^{13}C acetate and $^{13}CH_3$ methionine into colomitide C (**6**).

Table 2
^1H and ^{13}C data for **6**–**7** (CD_3OD, δ in ppm and J in Hz).

Position	**6**		**7**	
	δ_H	δ_C	δ_H	δ_C
1		216.3		204.5
2	2.83 q (6.6)	45.7	3.00 m	42.2
3	a 1.65 m b 1.37 m	28.0	a 1.59 m b 1.38 m	28.9
4	0.86 t (7.2)	12.0	0.86 t (8.1)	19.0
5	1.04 d (6.6)	16.8	1.06 d (6.6)	12.7
1′				
2′		110.1	4.26 m	77.9
3′	1.81 q (7.2)	43.9	1.60 m	37.9
4′	2.71 dd (4.2, 3.5)	43.4	2.63 m	37.6
5′	2.78 dd (4.8, 3.5)	54.0		118.6
6′	a 4.04 d (12.0) b 3.83 dd (12.0, 4.8)	60.1	7.90 s	160.6
7′	1.27 s	20.5	1.30 d (6.3)	20.2
8′	0.90 d (7.2)	14.4	1.10 d (7.0)	14.8
9′	a 4.17 dd (8.4, 4.2) b 4.00 d (8.4)	72.5	a/b 3.61 m	61.9

Table 5
Observed intensities of peak signals in ^{13}C NMR spectra for natural colomitide C, enrichments with [2- ^{13}C] acetate and [1- ^{13}C] acetate, and percent of ^{13}C incorporation for each position.

Position	δ_C(ppm)	Observed intensities			%^{13}C	
		Unlabeled	[2-^{13}C]	[1-^{13}C]	[2-^{13}C]	[1-^{13}C]
1	216.7	0.286	0.015	0.013	0.9	**1.8**
2	45.8	0.614	0.016	0.093	**32**	0.9
3	28.0	0.591	0.044	0.033	1.2	**2.6**
4	12.0	0.593	0.019	0.129	**4.6**	1.1
5	16.7	0.551	0.021	0.038	1.5	1.4
2′	110.2	0.389	0.017	0.013	0.7	**1.6**
3′	44.0	0.644	0.019	0.122	**4.0**	1.0
4′	43.4	0.555	0.036	0.028	1.1	**23**
5′	54.1	0.636	0.018	0.104	**3.5**	1.0
6′	60.2	0.619	0.037	0.030	1.0	**2.1**
7′	20.4	0.654	0.021	0.130	**4.2**	1.1
8′	14.4	0.605	0.021	0.041	1.4	1.2
9′	72.6	0.679	0.020	0.119	**3.7**	1.0

Bolded numbers indicate which labeled precursor was enriched.

Table 3
^1H and ^{13}C data for **8**–**10** (CD_3OD (a) and $CDCl_3$ (b), δ in ppm and J in Hz).

Position	**8**[a]		**9**[b]		**10**[b]	
	δ_H	δ_C	δ_H	δ_C	δ_H	δ_C
1		179.6		180.3		178.2
2	3.39 q (7.3)	35.3	3.45 m	34.2	2.39 m	42.7
3	a 1.56 m b 1.47 m	28.0	a 1.51 m b 1.41 m	27.3	a 1.65 m b 1.49 m	27.1
4	0.90 t (7.3)	12.0	0.86 t (7.5)	12.1	0.90 t (7.3)	12.2
5	1.09 d (7.3)	17.5	1.06 d (7.1)	17.9	1.13 d (6.9)	17.2
1′						
2′	4.44 q (6.9)	83.5		211.5	4.36 m	82.4
3′	2.00 m	33.4	3.04 m	48.3	1.97 m	36.9
4′	3.77 td (10.8, 4.8)	38.8	3.46 m	45.2	2.39 m	35.4
5′		97.3		102.7	a 2.65 dd (17.6, 6.6) b 2.49 dd (17.6, 5.8)	33.4
6′		166.2		171.3		174.4
7′	1.37 d (6.9)	21.2	2.13 s	30.7	1.37 d (6.2)	21.3
8′	0.98 d (7.4)	13.2	1.03 d (7.1)	13.9	1.06 d (7.0)	14.1
9′	a 4.67 dd (10.8, 9.9) b 4.21 dd (10.8, 9.9)	74.9	a 4.44 dd (9.5, 4.2) b 4.39 dd (9.5, 3.8)	73.9	a 4.20 dd (11.3, 5.5) b 4.13 dd (11.3, 5.5)	64.9

Table 4
^1H and ^{13}C data for **11**–**13** (CD_3OD (a) and DMSO-d_6 (b), δ in ppm and J in Hz).

Position	**11**[a]		**12**[b]		**13**[a]	
	δ_H	δ_C	δ_H	δ_C	δ_H	δ_C
1		168.2		209.7		215.5
2	3.55 m	35.0		50.8	2.48 m	49.6
3	a 1.55 m b 1.35 m	26.5	a/b 1.37 m	27.2	a 1.64 m b 1.35 m	27.4
4	0.86 t (7.8)	11.7	0.70 t (7.3)	9.4	0.85 t (7.4)	12.4
5	1.09 d (6.6)	17.6	0.92 s	20.6	1.03 d (6.9)	16.8
1′						
2′	4.32 q (6.6)	79.7	a 1.70 m b 1.55 m	25.9		214.2
3′	2.04 m	29.2	2.89 m	35.4	2.80 m	48.3
4′	3.38 m	46.0		178.0	2.75 m	35.7
5′		94.5		137.3	a/b 2.52 d (6.9)	40.5
6′		172.4	3.98 br.s	51.2	8.06 s	163.1
7′	1.25 d (6.6)	18.8	0.82 t (7.3)	12.3	2.17 s	29.4
8′	0.90 d (7.2)	12.5	1.18 d (7.3)	19.6	1.03 d (6.9)	12.9
9′	a 4.42 dd (9.0, 8.4) b 3.93 dd (9.6, 9.0)	68.0	4.31 d (6.6)	77.3	a 4.10 dd (11.0, 6.6) b 4.06 dd (11.0, 5.9)	66.1
OH-6′			4.59 br s			
OH-9′			5.34 d (6.6)			

4. Experimental

4.1. General experimental procedures

Optical rotations were measured on a Rudolph Research Analytical Autopol III polarimeter. IR spectra were obtained using a JASCO 4100 FT-IR spectrophotometer. Low and high resolution mass analyses were performed using an Agilent TOF II mass spectrometer with a dual ESI and APCI source. A JASCO 200 system was used to record the CD spectra. Standard 1D and 2D NMR spectra were recorded on a Varian 600 MHz spectrometer in CD_3OD. Proton and carbon chemical shifts are reported in ppm and referenced with the ^1H and ^{13}C signals of residual methanol or chloroform. Flash chromatography separations were performed using a Teledyne ISCO Combiflash Rf system. TLC separations were performed using Whatman silica gel 60 F_{254} aluminum backed TLC plates. Sephadex LH-20 (GE Healthcare) and silica gel 60 (230–400 mesh, Merck) were used as the stationary phases for column chromatography. HPLC separations were performed with an Agilent 1200 instrument with a PDA detector system. VCD spectra were recorded on a ChiralIR2X™ VCD spectrometer (BioTools, Inc.) equipped with dual PEM, 4 cm^{-1} resolution and optimized at 1400 cm^{-1}. Molecular modeling studies were performed using Avogadro 1.2 and Chem3D 15.0 and structures were energy minimized using the MMFF94 forcefield.

4.2. Microorganisms and culture conditions

The cultures used in these studies were isolated from samples that were collected during investigations to assess wood decay in historic structures of Antarctica. *Cadophora malorum* (UMN Di3-4, Genbank KF053544.1) and *Cadophora fastigiata* (UMN Di76-3, Genbank KF053563.1) were isolated from historic woods located at Deception Island, Antarctica (62° 58′S, 60° 39′W) (Held et al., 2011). *Cadophora luteo-olivacea* isolates, UMN PL12-3 (Genbank KF053556.1) and UMN 3E41-2 (Genbank AY371510), were isolated from wood sampled from a historic structure at British Base A on Goudier Island (*64° 49′S, 63° 30′W*), Port Lockroy on the Antarctic Peninsula and from wood at Robert F. Scott's historic hut at Cape Evans (*77° 38′S, 166°25′E*), Ross Island, Antarctica, respectively (Arenz and Blanchette, 2009). Cultures are maintained in the Forest Pathology live culture collection at the U of MN Department of Plant Pathology.

Small segments of wood were collected in sterile bags and kept at 4 °C until they were brought to the laboratory at the University of Minnesota. Fungi were isolated from the samples by culturing on malt extract media that contained 0.2% lactic acid as previously described. (Blanchette et al., 2010). Isolates were cultured at 20 °C and pure cultures obtained after subsampling. Fungi were identified by DNA sequencing of the internal transcribed spacer region using previously described methods (Blanchette et al., 2010).

4.3. Extraction, isolation and identification

A seed culture of *C. luteo-olivacea* was grown on a malt agar plate for 10 days which was then chopped into small pieces and vortexed in a 50 mL conical tube with 10 mL of PBS buffer. Approximately 10% of this agar suspension was used to inoculate each rice medium flask (twenty one x 1 liter flasks containing 100 g rice and 100 mLmL of water) which was cultured at room temperature for 30 days.

The rice cultures were exhaustively extracted with EtOAc and MeOH. Extracts were combined, concentrated and successively partitioned with 0.5 L of EtOAc, n-Hex and n-BuOH (3× for each solvent). The EtOAc fraction (~8 g) was purified by flash chromatography (Teledyne ISCO Combiflash® Rf; Solid phase Redisep® Rf 80 g silica; gradient elution 0–100% of EtOAc/n-Hex for 30 min; flow rate 40 mL/min). Fractions were pooled into 16 fractions (**F1**-**F16**) based on TLC analysis. From this step, **4** (61.2 mg) was isolated as a pure compound. Fraction **F2** (5.3 g) was further separated using flash chromatography (gradient elution 0–100% $MeOH/CH_2Cl_2$ for 30 min; flow rate 40 mL/min) to generate **1** (36.5 mg), **2** (41.9 mg), **3** (1.8 mg) and **6** (3365 mg). Sub-fraction **F2.53** was repurified using flash chromatography (Solid phase Redisep® Rf 40 g silica; gradient elution 0–100% of EtOAc/n-Hex for 30 min; flow rate 20 mL/min) to generate 28 subfractions (**F2.53.1** – **F2.53.28**). Subfraction **F2.53.20** was subjected to semi-preparative HPLC (reversed phase C18, mobile phase CH_3CN/H_2O, gradient elution 30% to 100%, 3 mLmL/minute for 30 min) to generate **5** (4.7 mg) and **12** (2.7 mg). Subfraction **F2.53.12** was purified by size exclusion chromatography (Sephadex LH-20) and two subsequent semi-preparative HPLC separations to yield pure compounds **7** (1.8 mg), **9** (1.5 mg), and **11** (1.8 mg). Compound **8** (1.1 mg), **10** (1.9 mg), and **13** (4.6 mg) were recovered after purification of fraction **F2.11A** using two subsequent semi-preparative HPLC separations (3 mLmL/minute gradient elution 5%–100% of CH_3CN/H_2O and 55%–100% of CH_3CN/H_2O on RP C-18 for 20 and 13 min, respectively).

4.3.1. Dihydrospiciferone A (*3*)

White solid; $[\alpha]^{25}_D$: +28° (*c* 0.2 in EtOH); UV (EtOH) λ_{max} (log ε) 205 (3.18), 220 (3.17), 230 (3.24), 245 (3.24), 260 (3.22); IR (film) ν_{max} 3896, 3847, 3791, 2965, 2107, 1661, 1818, 1054 cm^{-1}; For ^1H and ^{13}C NMR spectroscopic data, see Table 1; HRAPCI-MS m/z 235.1347 $[M+H]^+$ (calculated for $C_{14}H_{19}O_3$, 235.1329).

4.3.2. Spiciferone F (*5*)

White solid. $[\alpha]^{25}_D$: −160 (*c* 0.05 in MeOH); UV (MeOH) λ_{max} (log ε) 205 (3.37), 220 (3.37), 230 (3.43), 245 (3.44), 260 (3.42), 295 (3.41; IR (film) ν_{max} 3896, 3855, 3847, 3802, 3696, 3680, 2971 (sharp), 2863 (sharp), 2842, 2076, 1678, 1560, 1455, 1346, 1055, 1031, 1015 cm^{-1}; For ^1H and ^{13}C NMR spectroscopic data, see Table 1; HRAPCI-MS m/z 373.1653 $[M+H]^+$ (calculated for $C_{21}H_{25}O_6$, 373.1646).

4.3.3. Colomitide C (*6*)

Colorless oil; $[\alpha]^{25}_D$: +26 (*c* 0.1 in acetone); UV (MeOH) λ_{max} (log ε) 200 (3.02), 205 (2.88), 220 (2,48); IR (film) ν_{max} 3896, 3856, 3847, 3794, 3712, 7104, 1049, 1032 cm^{-1}; For ^1H and ^{13}C NMR spectroscopic data, see Table 2; HRAPCI-MS m/z 227.1653 $[M+H]^+$ (calculated for $C_{13}H_{23}O_3$, 227.1642). Volatility was determined by loss of mass over time with no apparent degradation.

4.3.4. Colomitide D (*7*)

Pale yellow oil; $[\alpha]^{25}_D$: −112(*c* 0.05 in MeOH); UV (MeOH) λ_{max} (log ε) 205 (3.15), 220 (3.13), 230 (3.21), 245 (3.21), 260 (3.19); IR (film) ν_{max} 3895, 3856, 3847, 3792, 3713, 3677, 2965, 1612, 1054, 1032, 1012 cm^{-1}; For ^1H and ^{13}C NMR spectroscopic data, see Table 2; HRAPCI-MS m/z 227.1662 $[M+H]^+$ (calculated for $C_{13}H_{23}O_3$, 227.1642).

4.3.5. Cadopherone A (*8*)

Colorless oil; $[\alpha]^{25}_D$: +60 (*c* 0.05 in MeOH); UV (MeOH) λ_{max} (log ε) 205 (3.15), 220 (3.14), 230 (3.21), 260 (3.19); IR (film) ν_{max} 3908, 3895, 3875, 3856, 3847, 3817, 3802, 3785, 3714, 3677, 2075, 1709, 1054, 1032 cm^{-1}; For ^1H and ^{13}C NMR spectroscopic data, see Table 3; HRAPCI-MS m/z 225.1484 $[M+H]^+$ (calculated for $C_{13}H_{21}O_3$, 225.1491).

*4.3.6. Cadopherone B (**9**)*

Colorless oil; $[\alpha]^{25}_D$: +48 (*c* 0.05 in MeOH); UV (MeOH) λ_{max} (log ε) 205 (3.19), 220(3.18), 225 (3.20); IR (film) ν_{max} 3895, 3856, 3847, 3802, 3714, 3678, 2965, 2842, 2077, 1709, 1455, 1379, 1054, 1032 cm^{-1}; For ^{1}H and ^{13}C NMR spectroscopic data, see Table 3; HRESIMS m/z 239.1274 [M-H]$^-$ (calculated for $C_{13}H_{19}O_4$, 239.1278).

*4.3.7. Cadopherone C (**10**)*

White solid; $[\alpha]^{25}_D$: −60 (*c* 0.05 in MeOH); UV (MeOH) λ_{max} (log ε) 205 (3.18), 220 (3.16), 230 (3.24), 245 (3.25); IR (film) ν_{max} 3896, 2825, 2068, 1054, 1032 cm^{-1}; For ^{1}H and ^{13}C NMR spectroscopic data, see Table 4; HRAPCI-MS m/z 243.1585 [M+H]$^+$ (calculated for $C_{13}H_{23}O_4$, 243.1596).

*4.3.8. Cadopherone D (**11**)*

Pale yellow solid; $[\alpha]^{25}_D$: +80 (*c* 0.05 in MeOH); UV (MeOH) λ_{max} (log ε) 205 (3.13), 230 (3.00), 240 (2.99); IR (film) ν_{max} 3895, 3856, 3847, 3802, 3745, 2964, 2067, 1745, 1654, 1032, 1005 cm^{-1}; For ^{1}H and ^{13}C NMR spectroscopic data, see Table 4; HRAPCI-MS m/z 225.1481 [M+H]$^+$ (calculated for $C_{13}H_{21}O_3$, 225.1491).

*4.3.9. Similin C (**12**)*

Pale Yellow oil; $[\alpha]^{25}_D$: +64 (*c* 0.05 in MeOH); UV (MeOH) λ_{max} (log ε) 205 (3.16), 230 (3.22), 245 (3.22); IR (film) ν_{max} 3896, 3866, 3856, 3847, 3790, 3745, 2108, 1687, 1032 cm^{-1}; For ^{1}H and ^{13}C NMR spectroscopic data, see Table 3; HRAPCI-MS m/z 227.1647 [M+H]$^+$ (calculated for $C_{13}H_{23}O_3$, 227.1642).

*4.3.10. Spicifernin B (**13**)*

Reddish yellow oil; $[\alpha]^{25}_D$: −112 (*c* 0.05 in MeOH); UV (MeOH) λ_{max} (log ε) 200 (3.17), 235 (2.96), 260 (3.14); IR (film) ν_{max} 3895, 3856, 3847, 3801, 2965, 2108, 1707 (sharp), 1457, 1376, 1166, 1056, 1032, 1006 cm^{-1}; For ^{1}H and ^{13}C NMR spectroscopic data, see Table 4; HRAPCI-MS m/z 243.1608 [M+H]$^+$ (calculated for $C_{13}H_{22}O_4$, 243.1596).

4.4. VCD analysis

A conformational search was carried out with Compute VOA for each configuration of colomitide C (**6**) at the MMFF94 level. For each configuration, geometry optimization, frequency, and IR and VCD intensity calculations of the conformers resulted from the conformational search were carried out at the DFT level (B3LYP functional/6−31 G(d) basis set) with Gaussian 09 (Gaussian Inc., Wallingford, CT). The calculated frequencies were scaled by 0.973 and the IR and VCD intensities were converted to Lorentzian Bands with 6-cm^{-1} half-width for comparison to experimental values.

4.5. ^{13}C feeding experiment

A culture was prepared by autoclaving 100 g rice and 500 μg [2−^{13}C] sodium acetate or 200 μg [1−^{13}C] sodium acetate with 100 mL water and inoculating with approximately 10% of a well grown malt agar plate of *C. luteo-olivacea* cut into small pieces and vortexed with PBS. Ten mLs of [2−^{13}C] sodium acetate (50 mg/mL) or [1−^{13}C] sodium acetate (20 mg/mL) was added onto the surface of the medium every five days (days 5, 10, 15, 20 and 25) before harvesting on day 30 (Pathre et al., 1989). Extracts were made and compounds purified with the same methods used to obtain the original spiciferone and colomitide compounds. The relative enrichment of ^{13}C for each carbon was determined using the methods of Canham et al. (1976, 1977). The ratio *R* was calculated as the intensity of each signal in the NMR spectrum divided by the intensity of a single unlabeled reference peak in the same spectrum. The ratio *r* was then determined by dividing the value of *R* (labeled spectrum) by *R* (natural abundance spectrum). The percentage of ^{13}C incorporation was calculated by multiplying each value of *r* by a scaling factor necessary to convert the average peak intensity of unlabeled carbons in the spectrum to 1.108% (^{13}C natural abundance).

4.6. Biological assays

4.6.1. Antimicrobial assays

Compounds were tested against the following panel of bacteria and fungi purchased from the American Type Culture Collection (ATCC): Methicillin-resistant *Staphylococcus aureus* (MRSA) ATCC 43300, vancomycin-resistant *Enterococcus faecalis* (VRE) ATCC 51299, *Bacillus subtilis* ATCC 6633, *Escherichia coli* ATCC 25922, *Acinetobacter baumannii* ATCC 19606, *Pseudomonas aeruginosa* ATCC 27853, *Klebsiella pneumonia* ATCC 13883, *Cryptococcus neoformans* ATCC 66031 and *Candida albicans* ATCC 10231. MRSA, *B. subtilis*, *A. baumannii*, *P. aeruginosa*, *E. coli*, and *K. pneumoniae* were grown in BBL™ Trypticase™ Soy Broth (BD) at 37 °C. VRE was grown in brain heart infusion broth (Bacto) at 37 °C and *C. albicans* and *C. neoformans* were grown in yeast malt extract medium (Difco) and Sabouraud dextrose broth (Difco), respectively, at 30 °C.

Microbial susceptibility testing was performed using an adaptation of the standard microbroth dilution assay (Performance standards for antimicrobial susceptibility testing, 2011). Briefly, bacteria were grown to mid-log phase, diluted with fresh medium to an optical density at 600 nm (OD_{600}) of 0.030−0.060 and then diluted again 1:10. This suspension (195 μL) was added to wells in a 96 well microtiter plate (Sarstedt) and 5 μL of compound dissolved in DMSO was added to give a final concentration of 100−0.1 μM at 2.5% DMSO by volume. A DMSO negative control and standard antibiotic positive controls were included in each plate. All compounds were tested in triplicate for each concentration. Plates were sealed with parafilm, placed in a Ziploc bag to prevent evaporation, and incubated at 30 °C (fungi) or 37 °C (bacteria) for 16−20 h (48 h for *C. neoformans*). The OD_{600} values for each well were determined with a plate reader (Biotek, EL800) and the data were standardized to the DMSO control wells after subtracting the background from the blank media wells.

4.6.2. MTT cell viability (cytotoxicity)

Cytotoxicity of each compound was determined with a standard tetrazolium assay using SF-295 glioblastoma and LOX IMVI melanoma cancer cell lines (Denizot and Lang, 1986; Mossman, 1983). LOX IMVI and SF-295 cells were maintained in growth media: RPMI 1640 (Invitrogen 11875-119) supplemented with 10% FBS (Invitrogen 16000-044), 1% Penicillin/Streptomycin (Invitrogen 15140-122) and 1% Glutamax-1 (Invitrogen 35050-061). Cells were plated in 96-well plates at 25×10^4 cells/mLmL. After 24 h, compounds were added at 9, 3× dilutions from 100 μM final concentration in growth media. Plates were incubated for 72 h at 37 °C in a 5% CO_2/95% air humidified atmosphere after which time the media was removed and MTT was added in RPMI phenol red free media. The MTT was removed after 3 h and formazan crystals were solubilized with 200 μL of isopropanol. Plates were read on a Molecular Devices SpectraMax i3 spectrophotometer at 570 nm for formazan and 690 nm for background subtraction. Percent viability was calculated using GraphPad Prism software.

Acknowledgments

This research is supported in part by National Science Foundation grant #PLR0537143 to R. Blanchette. This work was also supported in part by the Center for Drug Design. We are grateful to J. Gloer, C. Aldrich, and M. Gearhart for helpful discussions, and to H.

Irwin and J. Williams for conducting biological assays.

Appendix A. Supplementary data

Supplementary data related to this article can be found at https://doi.org/10.1016/j.phytochem.2017.12.019.

References

Almeida, C., Eguereva, E., Kehraus, S., Siering, C., Konig, G.M., 2010. Hydroxylated sclerosporin derivatives from the marine-derived fungus *Cadophora malorum*. J. Nat. Prod. 73 (3), 476–478.

Arenz, B.E., Blanchette, R.A., 2009. Investigations of fungal diversity in wooden structures and soils at historic sites on the Antarctic peninsula. Can. J. Microbiol. 55 (1), 46–56.

Blanchette, R.A., Held, B.W., Jurgens, J.A., McNew, D.L., Harrington, T.C., Duncan, S.M., Farrell, R.L., 2004. Wood-destroying soft rot fungi in the historic expedition huts of Antarctica. Appl. Environ. Microbiol. 70 (3), 1328–1335.

Blanchette, R.A., Held, B.W., Jurgens, J.A., 2008. Northumberland house, fort conger and the peary huts in the Canadian high arctic: current condition and assessment of wood deterioration taking place. In: Barr, S., Chaplin, P. (Eds.), Historical Polar Bases – Preservation and Management. International Polar Heritage Committee, Oslo, Norway, 96 pp.

Blanchette, R.A., Held, B.W., Arenz, B.E., Jurgens, J.A., Baltes, N.J., Duncan, S.M., Farrell, R.L., 2010. An Antarctic hot spot for fungi at shackleton's historic hut on Cape Royds. Microb. Ecol. 60 (1), 29–38.

Canham, P., Vining, L.C., Mcinnes, A.G., Walter, J.A., Wright, J.L.C., 1976. Pattern of acetate incorporation into aglycone ofchartreusin – evidence from C-13 nuclear magnetic-resonance studies for asingle-chain polyketide intermediate. J.Chem. Soc. Chem. Commun. 9, 319–320.

Canham, P.L., Vining, L.C., Mcinnes, A.G., Walter, J.A., Wright, J.L.C., 1977. Use of C-13 in biosynthetic-studies. incorporation of C-13-labeled acetate into chartreusin by *Streptomyces chartreusis*. Can. J. Chem. Rev. Canad. De Chim. 55 (12), 2450–2457.

Chan, Y.A., Podevels, A.M., Kevany, B.M., Thomas, M.G., 2009. Biosynthesis of polyketide synthase extender units. Nat. Prod. Rep. 26 (1), 90–114.

Denizot, F., Lang, R., 1986. Rapid colorimetric assay for cell-growth and survival - modifications to the tetrazolium dye procedure giving improved sensitivity and reliability. J. Immunol. Meth. 89 (2), 271–277.

Dong, J., Wang, L., Song, H., Shen, K., Zhou, Y., Wang, L., Zhang, K., 2009. Colomitides A and B: novel ketals with an unusual 2,7-dioxabicyclo [3.2.1]octane ring system from the aquatic fungus YMF 1.01029. Chem. Biodiv. 6 (8), 1216–1223.

Edrada, R.A., Wray, V., Berg, A., Grafe, U., Sudarsono, Brauers G., Proksch, P., 2000. Novel spiciferone derivatives from the fungus *Drechslera hawaiiensis* isolated from the marine sponge *Callyspongia aerizusa*. Z Naturforsch C 55 (3–4), 218–221.

Held, B.W., Arenz, B.E., Blanchette, R.A., 2011. Factors influencing deterioration of historic structures at Deception island, Antarctica. In: Barr, S., Chaplin, P. (Eds.), Polar Settlements - Location, Techniques and Conservation. ICOMOS Monuments and Sites. International Polar Heritage Committee, Oslo, Norway, p. 35, 43 pp.

Hwang, I.H., Swenson, D.C., Gloer, J.B., Wicklow, D.T., 2016. Disseminins and spiciferone analogues: polyketide-derived metabolites from a fungicolous isolate of *Pestalotiopsis disseminata*. J. Nat. Prod. 79 (3), 523–530.

Jurgens, J.A., Blanchette, R.A., Filley, T.R., 2009. Fungal diversity and deterioration in mummified woods from the Ad Astra ice cap region in the Canadian high arctic. Polar Biol. 32 (5), 751–758.

Kinzer, G.W., Fentiman Jr., A.F., 1969. Bark beetle attractants: identification, synthesis and field bioassay of a new compound isolated from *Dendroctonus*. Nat. Lon. 221, 477–478.

Mossman, T., 1983. Rapid colorimetric assay for cellular growth and survival - application to proliferation and cytotoxicity assays. J. Immunol. Meth. 65 (1–2), 55–63.

Nakajima, H., Hamasaki, T., Kimura, Y., 1989. Structure of spiciferone-A, a novel gamma-pyrone plant-growth inhibitor produced by the fungus *Cochliobolus spicifer* Nelson. Agric. Biol. Chem. 53 (8), 2297–2299.

Nakajima, H., Hamasaki, T., Maeta, S., Kimura, Y., Takeuchi, Y., 1990. A plant-growth regulator produced by the fungus, *Cochliobolus spicifer*. Phytochemistry 29 (6), 1739–1743.

Nakajima, H., Matsumoto, R., Kimura, Y., Hamasaki, T., 1992. Biosynthesis of spicifernin, a unique metabolite of the phytopathogenic fungus, Cochliobolus spicifer. J. Chem. Soc. Chem. Comm. (22), 1654–1656.

Nakajima, H., Fujimoto, H., Kimura, Y., Hamasaki, T., 1993a. Importance of the ketone function for the phytotoxicity of spiciferone-A, a phytotoxin produced by the fungus *Cochliobolus spicifer*. Biosci. Biotechnol. Biochem. 57 (11), 1938–1939.

Nakajima, H., Fujimoto, H., Matsumoto, R., Hamasaki, T., 1993b. Biosynthesis of spiciferone-a and spicifernin, bioactive metabolites of the phytopathogenic fungus, *Cochliobolus spicifer*. J. Org. Chem. 58 (17), 4526–4528.

Nakajima, H., Fukuyama, K., Fujimoto, H., Baba, T., Hamasaki, T., 1994. Absolute stereochemistry of spiciferones and spicifernin, bioactive metabolites of the fungus *Cochliobolus spicifer* - evidence for their unique biosynthesis. J. Chem. Soc. Perk. Trans. 1 (13), 1865–1869.

Pathre, S.V., Khadikar, P.V., Mirocha, C.J., 1989. Biosynthesis of zearalenone - a simple and efficient method to incorporate [C-13]acetate label by using solid cultures. Appl. Environ. Microbiol. 55 (8), 1955–1956.

Performance standards for antimicrobial susceptibility testing: 14th informational supplement, 2011. Performance Standards for Antimicrobial Susceptibility Testing: 14th Informational Supplement Nat Comm Clin Lab Stand, vol. 21. M100–S14.

Rusman, Y., Held, B.W., Blanchette, R.A., Wittlin, S., Salomon, C.E., 2015. Soudanones A-G: antifungal isochromanones from the ascomycetous fungus *Cadophora* sp. isolated from an iron mine. J. Nat. Prod. 78 (6), 1456–1460.

Silverstein, R.M., Brownlee, R.G., Bellas, T., Wood, D.L., Browne, L., 1968. Brevicomin: principal sex attractant in the frass of the female western pine beetle. Science 159 (3817), 889–891.

Song, L., Barona-Gomez, F., Corre, C., Xiang, L., Udwary, D.W., Austin, M.B., Noel, J.P., Moore, B.S., Challis, G.L., 2006. Type III polyketide synthase beta-ketoacyl-ACP starter unit and ethylmalonyl-CoA extender unit selectivity discovered by *Streptomyces coelicolor* genome mining. J. Am. Chem. Soc. 128 (46), 14754–14755.

Spadaro, D., Galliano, A., Pellegrino, C., Gilardi, G., Garibaldi, A., Gullino, M.L., 2010. Dry matter, mineral composition, and commercial storage practices influence the development of skin pitting caused by *Cadophora luteo-olivacea* on kiwifruit 'hayward'. J. Plant Pathol. 92 (2), 349–356.

Sugar, D., Spotts, R.A., 1992. Sources of inoculum of *Phialophora malorum*, causal agent of side rot of pear. Phytopathology 82 (7), 735–738.

Travadon, R., Lawrence, D.P., Rooney-Latham, S., Gubler, W.D., Wilcox, W.F., Rolshausen, P.E., Baumgartner, K., 2015. *Cadophora* species associated with wood-decay of grapevine in North America. Fungal Biol. 119 (1), 53–66.

Weber, H., Swenson, D., Gloer, J., Malloch, D., 1992. Similin-a and similin-B - new antifungal metabolites from the coprophilous fungus *Sporormiella similis*. Tetrahedron Lett. 33 (9), 1157–1160.

Yang, H., Liu, X., Li, X., Shi, X., Yang, F., Jiao, X., Xie, P., 2017. Enantioselective total synthesis of colomitides and their absolute configuration determination and structural revision. Org. Biomol. Chem. 15 (17), 3728–3735.